

Three-Dimensional Measurement Technologies for Advanced Manufacturing

● Hiroyuki Tsukahara

(Manuscript received May 31, 2006)

Three-dimensional (3D) measurement is a very important elemental technology in manufacturing. Because of the increasingly fine structures of modern components, this technology must be extremely fast and accurate. At Fujitsu, because we manufacture semiconductors, hard disk drives, display elements, and micro electro mechanical systems (MEMS) devices, 3D measurement technology that enables fast, accurate measurement of solid shapes in the sub-micron to sub-nanometer region has become essential. In this paper, we introduce examples of how triangulation and optical interferometry are used in the 3D measurement technologies that have been developed so far and then look at some future developments. First, we describe a high-speed solder bump-height measurement system that uses triangulation. Next, we describe technologies that use optical interferometry to measure the slider ABS and disk micro-waviness of magnetic disks and the light-guiding plates for display elements. Finally, we introduce a technology for measuring the dynamic behavior of MEMS devices.

1. Introduction

Three-dimensional (3D) measurement is a very important elemental technology in electronics manufacturing. Because electronic components have extremely fine structures and are manufactured in large numbers, the development of measurement technology must take both precision and speed into account. At Fujitsu, because we manufacture semiconductors,¹⁾ hard disk drives (HDDs),²⁾ display elements, and micro electro mechanical systems (MEMS) devices, 3D measurement technology that enables fast, accurate measurement of solid shapes in the sub-micron to sub-nanometer region has become essential.

In this paper, we introduce some examples of 3D measurement technologies based on triangulation and optical interferometry that we have developed. The examples are a solder bump measurement technology used in semiconductor

mounting, technologies for measuring the surface shape of magnetic head sliders and the micro-waviness of magnetic disks, and a technology for measuring the light-guiding plates used in display modules. Finally, we introduce a technology for measuring the dynamic behavior of MEMS devices, a recent focus area, and then look at some future developments.

2. Three-dimensional measurement technology for semiconductor mounting

In this section, we introduce a high-speed bump-height measurement technology that is used in semiconductor mounting as an example of 3D measurement technology based on triangulation.

Today's advanced high-density, high-speed LSIs can have thousands of high-speed external input-output signal electrodes, and the flip-chip

mounting method, which connects LSI chips directly to the wiring board without packages, has been adopted for mounting these devices. In this mounting method, a large number of electrodes can be positioned in a grid pattern on the surface of the LSI chip. Solder bumps are then formed on top of the electrodes so they can be directly connected to the wiring board. The normal bump shape is spherical, with a diameter from 50 to 150 μm and a height from 50 to 100 μm . A scanning electron microscope (SEM) photograph of the bumps on an LSI is shown in **Figure 1**.³⁾ This LSI is 17 \times 17 mm and has 11 000 bumps at a pitch of 150 μm .

In solder junctions, in addition to fatal defects such as electrical disconnections and shorts, latent defects such as potential disconnections and potential shorts also occur. After long-term use, there is a risk that these latent defects will become fatal defects. With the earlier, conventional method of mounting LSIs onto packages, the junction areas could still be seen after soldering. Therefore, a visual check could be done to find fatal or latent flaws. However, with the flip-chip mounting method, the space between the LSI chip and the wiring board is too narrow to permit a visual check of the junction area. Checking is therefore done by measuring the height of the solder bumps before mounting

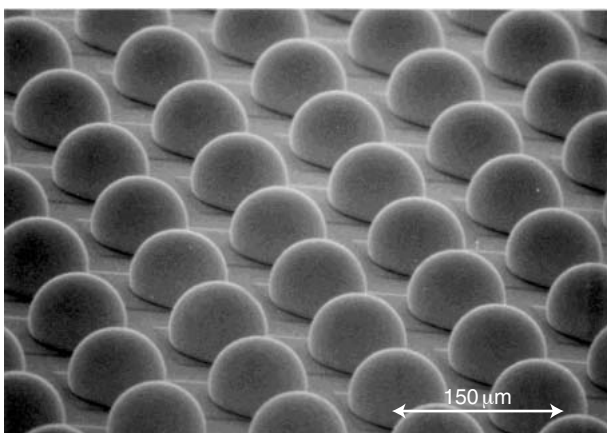


Figure 1
Solder bumps.

and then ascertaining whether the bumps fall within the standard. To do this, we developed a technology for high-speed bump-height measurement.⁴⁾⁻⁶⁾

The arrangement of the 3D high-speed bump-height sensing system is shown in **Figure 2**. We used triangulation to achieve high-speed measurement of bump height. A laser beam obliquely illuminates the bumps, and a one-dimensional position-sensitive detector (PSD) measures their height by detecting the difference in height between the laser beam reflected from the bump apexes and the laser beam reflected from the surface of the LSI. When the reflected laser beam is refocused onto the PSD sensor, a photocurrent is generated at that position. The photocurrent values output from the electrodes at the sides of the PSD are inversely proportional to the distance between the refocused beam and the electrodes. Moreover, the strength of the refocused beam can be found by summing the photocurrents. Accordingly, the position of the refocused beam between the PSD electrodes can be found by normalizing the difference in photocurrents with the strength of the refocused beam (**Figure 2**).

If the laser light does not hit the bump apex because the solder bump is hemispherical, the bump height cannot be measured correctly. To solve this problem, we incorporated a laser scanning unit in the optical system to detect the height of the entire upper area of the LSI, including the bump apexes. As shown in **Figure 2**, an acousto-optical deflector (AOD) is used in the laser scanning unit to scan the semiconductor laser light. The scanning length of this optical system is 1 mm. Accordingly, by moving the target LSI in a straight line, height and brightness images of 1 mm \times the distance moved can be obtained simultaneously. Examples of height and brightness images are shown in **Figure 3**. **Figure 3(a)** shows a PSD brightness image, and **Figure 3(b)** shows a PSD height image. The width of these images corresponds to the scanning length, which is 1 mm. Because the PSD optical system only

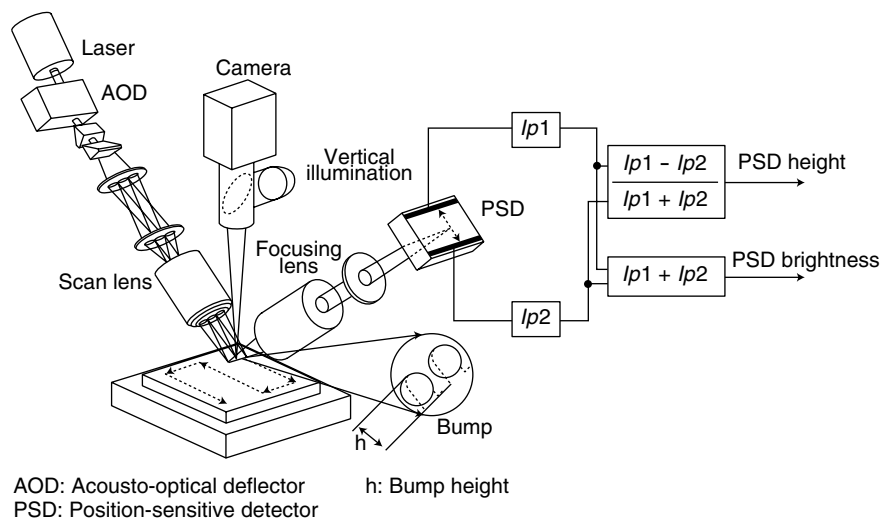


Figure 2
 High-speed bump-height sensing system.

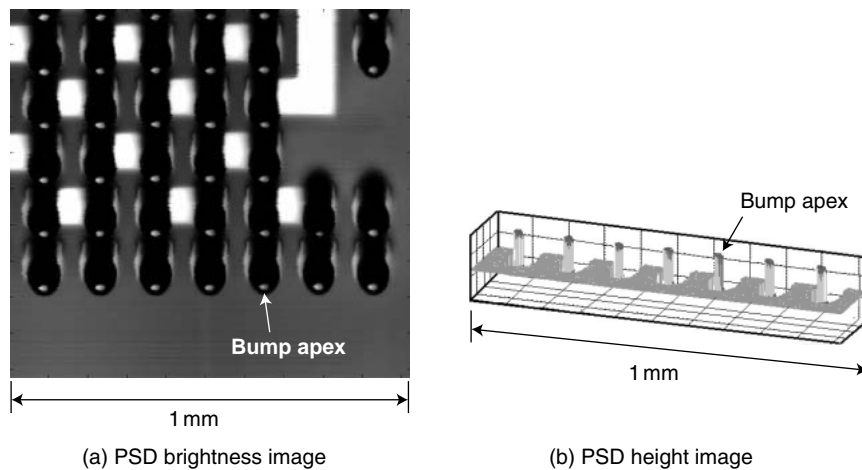


Figure 3
 Measurement of solder bumps.

receives light from the bump apices, bright points can be seen in the dark elliptical shapes in the brightness image. In the height image, the heights of these bright points, and hence the heights of the apices, are detected.

We used this system to measure the heights of 1300 bumps about 60 to 70 μm in height and then repeated the measurements using a toolmaker's microscope. **Figure 4** compares the results of these measurements. We found there was a

satisfactory correlation between these measurements, and a measurement precision (average σ) of within $\pm 0.25 \mu\text{m}$ was realized.

A wafer-bump inspection system that uses the detection and measurement technology we developed is shown in **Figure 5**. As well as being able to measure solder bumps on 6-inch to 8-inch wafers, this equipment can also be used to measure Au-plated bumps and Cu posts in chip scale packages (CSPs).

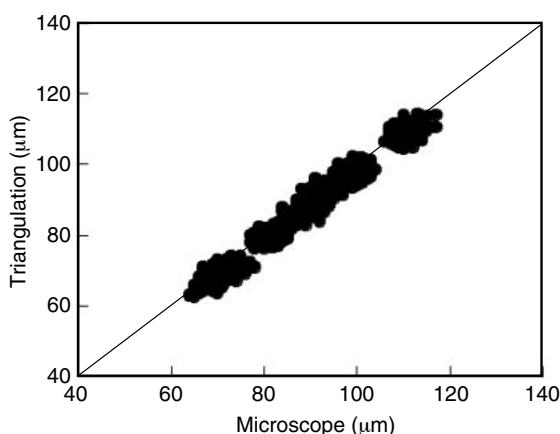


Figure 4
Bump-height measurement comparison.



Figure 5
Wafer-bump inspection system.

3. Three-dimensional measurement technology for hard disk drives

In this section, we introduce some example applications of optical interferometry for 3D measurements of hard disk drives (HDDs).

The increasingly higher recording densities of HDDs are achieved in part by reducing the flying height, which is the space between the magnetic head and the disk (**Figure 6**). Recently, the flying height has dropped below 10 nm.⁷⁾ To maintain a constant flying height, surface fluctuations must be minimized. The shape of the slider's air bearing surface (ABS) and the micro-waviness of the disk surface are the primary factors that affect the flying height of the magnetic head. We therefore developed technologies to measure a slider's ABS shape and disk micro-waviness.

3.1 Slider ABS shape measurement technology

The ABS determines the magnetic head's flying height characteristic, and because of the increasingly higher densities of magnetic disks, an inspection of the surface shape has become essential. Moreover, to improve the defect rate, slider adjustment may be required depending on

the shape. We therefore developed an ABS shape measurement technology that is suitable for use with a slider adjustment machine. The purpose of this technology is to perform high-speed, high-precision measurement of a slider's topography; find the crown, camber, and twist (CCT) curve parameters; and provide the adjustment machine with the surface data it requires to perform adjustment. In addition to speed and precision, which are basic measurement performance criteria, another important criterion is the realization of vibration tolerance when the slider ABS shape measurement technology is installed in the adjustment machine.

In the optical interference measurement field, phase-shifting interferometry has become widespread.⁸⁾ Phase-shifting interferometry extracts the interference phase that contains height data of each point from multiple interference fringe images. This method provides superior spatial resolution; however, because multiple interference images are required for each measurement, measurement takes time. Also, its measurement performance gradually decreases due to the vibrations that occur while the interference images are being captured. To solve these problems, we focused on the spatial carrier method⁹⁾ and developed a technology that enables

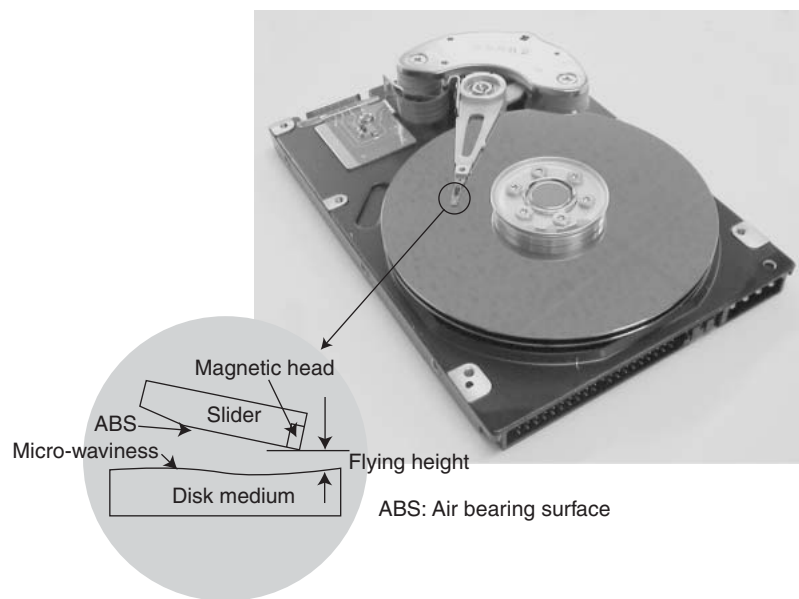


Figure 6
Hard disk drive.

one-step ABS topography measurement from the interference image of a slider (Figure 7).^{10),11)} This technology enables us to realize a measurement reproducibility (σ) of 0.1 nm; a high-precision, high-speed measurement time of 1 second per slider; and a measurement system that is not adversely affected by vibrations.

On the other hand, the positions in which the sliders under test were loaded on the tray were not uniform, so the interference fringe that was initially observed was not always suitable for measurement. We therefore determined the optimum interference fringe conditions for surface measurement by studying the relationship between the slider positions and the interference fringe spatial frequency and developed a technology for adjusting the slider positions so the interference fringe spatial frequency is always constant.^{10),11)} This technology enables automatic correction of the positions of the sliders on the tray and high-speed measurement of all the sliders. The slider ABS shape measurement system is shown in Figure 8.



(a) Carrier fringe image

(b) Slider ABS

Figure 7
Measurement of slider ABS topography.

3.2 Disk micro-waviness measurement technology

Micro-waviness refers to surface cycles ranging from 80 μm to several mm and causes fluctuations in flying height because the head cannot follow these variations in disk topography. Generally, a contact probe profilometer or an interferometric microscope is used to measure micro-waviness. However, the probe method can damage the disk and the interferometric microscope's narrow field of view makes the

measurement of micro-waviness, which has longer cycles than surface roughness, impossible. We therefore developed a technology for high-speed measurement of micro-waviness amplitude over the entire surface of a disk.^{12),13)}

Because measurement must be performed while the disk is rotating, we used the spatial carrier method here as well to perform one-shot interferometry. We developed a technology for dynamically measuring the micro-waviness of a disk's surface by interlinking the height interference images obtained from the rotating disk. By overlapping parts of adjacent interference images and linking the fields of view so the heights of the overlapped parts matched, we were able to



Figure 8
Slider ABS shape measurement system.

cancel out the vibrations that occurred during disk rotation and achieve high-precision measurement.

Examples of measured micro-waviness in two types of disks from different generations are shown in **Figure 9**. A 20 mm section from the height of one disk rotation (equivalent to 60 captured images) has been extracted and displayed. As can be seen, the newer-generation disk has less micro-waviness. The micro-waviness measurement system is shown in **Figure 10**.

4. Three-dimensional measurement technology for light-guiding plates of displays

In this section, we introduce the light-guiding plate, which is a component used for illumination in LCD devices, as another example of 3D measurement technology based on optical interferometry.

Figure 11 shows a prism-array light-guiding plate that is used in the display section of mobile products such as mobile phones. Because light-guiding plates are made using injection molding, the metal mold is also a measurement target. The measurement parameters are the surface roughness and outer dimensions. The surface roughness ranges from several nm to several 10s of nm and must be within the phase-shifting interferometer's measurement range, which is about 300 nm. However, because an allowance had to be made for a step height of around 10 μm in the outer dimensions, an

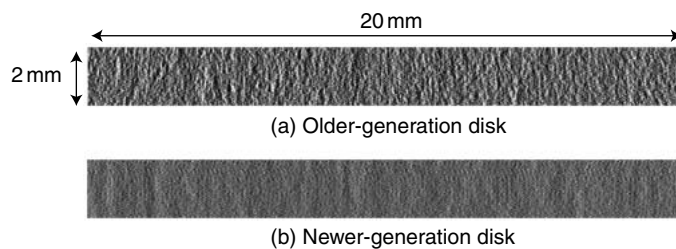


Figure 9
Measurement of disk micro-waviness.

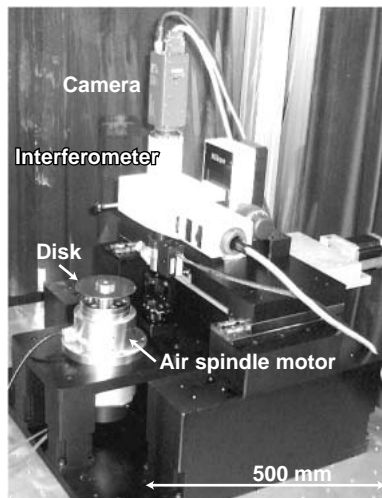


Figure 10
Micro-waviness measurement system.

expansion of the measurement range was required.

In phase-shifting interferometry, height variations that exceed the measurement range are wrapped and observed. Normally, the spatial continuity unwrapping method is employed. However, this method is not suitable for a structure such as a light-guiding plate, which has discrete steps. Two-wavelength phase-shifting interferometry, in which two light sources with slightly different wavelengths are used, is an accepted method of extending the measurement range of a phase-shifting interferometer.¹⁴⁾⁻¹⁷⁾ There are two types of two-wavelength phase-shifting interferometry: synthesized wavelength and fringe order determination. In the synthesized wavelength type, the measurement range is extended by synthesizing a long wavelength from two wavelengths. In the fringe order determination type, the measurement range is extended by finding the order of the interference fringe.

We selected the fringe-order determination type of two-wavelength phase-shifting interferometry because it can provide the same measurement accuracy as single-wavelength phase-shifting interferometry. However, this method is extremely susceptible to noise interference such as

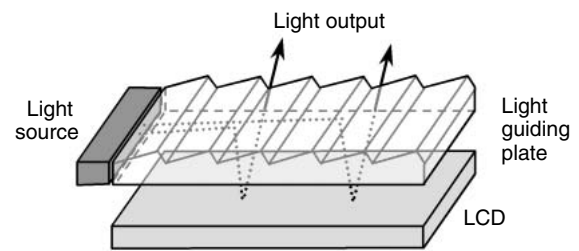


Figure 11
LCD display unit.

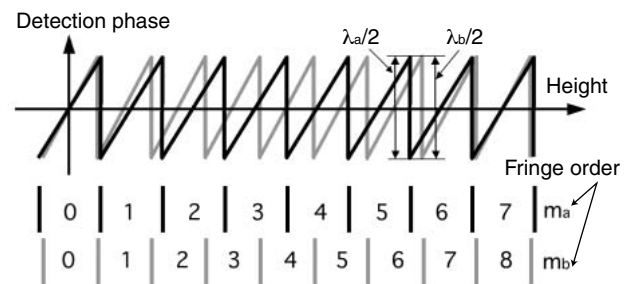


Figure 12
Relationship between height and fringe order.

vibrations, and because there is a considerable loss in measurement precision when used in general environments such as manufacturing plants, we were not able to find any examples of this method being used in measuring devices. We therefore decided to analyze the main causes of measurement error in two-wavelength phase-shifting interferometry and increase the noise tolerance.

The fringe-order determination type of two-wavelength phase shifting interferometry uses the amount of mutual phase shift extracted from each wavelength as a basis for calculating the number of cycles that each phase has shifted from the reference point, that is to say the fringe order at each point. The height calculation is then taken into account when the measurement range is extended (**Figure 12**). The deterioration in measurement precision of the fringe-order determination type of two-wavelength phase shifting interferometer is caused by the fringe-order error due to accumulated calculation errors. Fringe orders are calculated as real numbers and then

rounded to the nearest integer. After considering the calculation algorithm, we deduced that the error caused by this rounding down has a constant relationship with the main causes of fringe-order error; namely, the light source wavelength error and the initial phase difference between the two wavelengths. We then used this relationship to develop a new algorithm to find the light source wavelength error and the initial phase difference between the two wavelengths from the error histogram of the entire field of view. This algorithm enabled us to reduce the fringe-order error and also detect and correct generated errors.¹⁷⁾⁻¹⁹⁾ We used the Step Height Standard (a VLSI Standards Incorporated product) to evaluate the absolute measured values of this technology. The results are shown in **Table 1**. Because all of the measured values were step-height standard

values ranging from 8 to 8000 nm and fell within the uncertainty range of the Step Height Standard, we confirmed that this technology enabled the measurement range to be extended while maintaining the measurement precision of single-wavelength phase-shifting interferometry. This technology enables the simultaneous measurement of the outer dimensions and surface roughness of light-guiding plates and metal molds. Example measurements of the outer dimensions and surface roughness of a metal mold for a light-guiding plate are shown in **Figure 13 (a)** and **13 (b)**, respectively. The light-guiding plate and metal mold measurement system are shown in **Figure 14**.

5. Three-dimensional dynamic behavior measurement technology for MEMS devices

In this section, we introduce a technology for measuring the dynamic behavior of MEMS devices as an example of 3D measurement technology for measuring dynamic characteristics in the nanometer region.

In recent years, advances have been made in the use of MEMS devices in fields such as light scanners, acceleration sensors, and RF switches.²⁰⁾ In keeping with this trend, demands for technology that enables the observation of shape variations in a nanometer-region MEMS device while it is operating have increased. In response to these demands, we developed a technology for measuring the dynamic behavior of MEMS devices. Here,

Table 1
Evaluation of absolute step height values.

No.	Samples		Measurement		
	Certified height (nm)	Uncertainty (nm)	Height (nm)	Repeatability (nm)	Ratio (%)
1	9.0	0.5	9.1	0.05	0.55
2	46.4	0.7	46.6	0.11	0.24
3	84.9	1.1	84.7	0.15	0.18
4	182.3	2.0	182.0	0.14	0.08
5	459.1	2.7	459.7	0.13	0.02
6	939.5	5.6	937.6	0.12	0.01
7	956.8	5.8	959.7	0.10	0.01
8	1859	11	1851.2	0.58	0.03
9	7823	64	7845.9	0.62	0.01

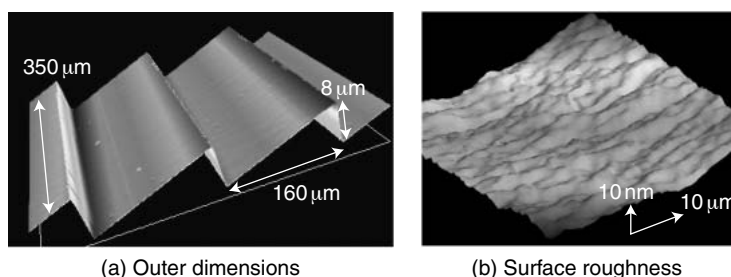


Figure 13
Measurements of metal mold for light-guiding plate.

we introduce the dynamic deformation measurement technology used in a MEMS light scanner. A photograph of the MEMS light scanner is shown in **Figure 15**.²¹⁾ The MEMS light scanner is a mechanical component used to scan laser light and replaces the earlier galvanometer mirrors and polygon mirrors. It is operated by applying torque to the mirror via torsion bars that are moved by generating an electrostatic force between comb electrodes. Deforming the mirror also deforms the scanning beam; therefore, the mirror's dynamic deformation must be measured and applied to the

design.

Since the MEMS light scanner operates in cycles, we developed a measurement technology that uses stroboscopic phase-shifting interferometry²²⁾⁻²⁴⁾ to synchronize with these cycles and generate strobes for interference measurement. Because the period during which strobe light generation can be measured is determined by the operating speed of the MEMS device, we employed a high-output laser diode (LD) to generate short light pulses. The maximum measurement speed is 100 km/h.



Figure 14
Light-guiding plate and metal mold measurement system.

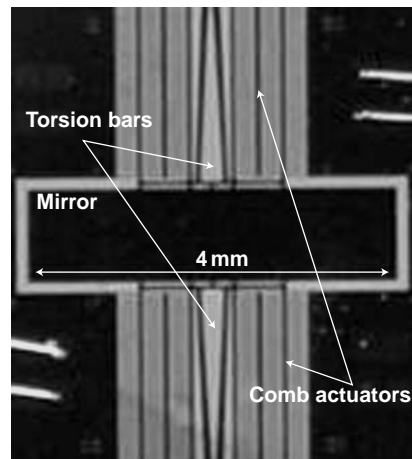


Figure 15
Photograph of MEMS scanning mirror.

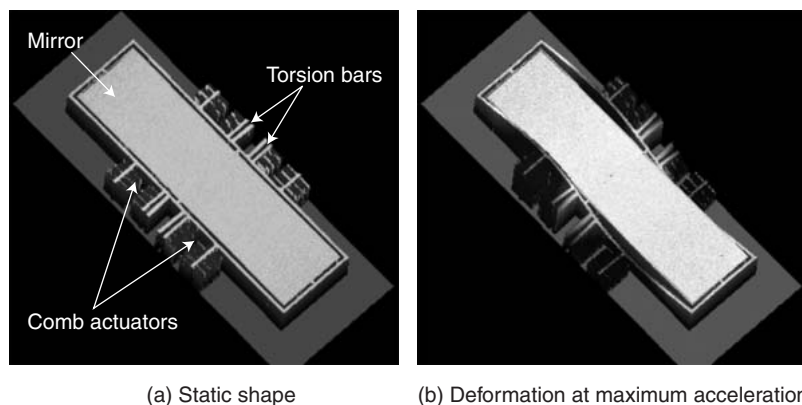


Figure 16
Static shape and dynamic deformation of MEMS light scanner.

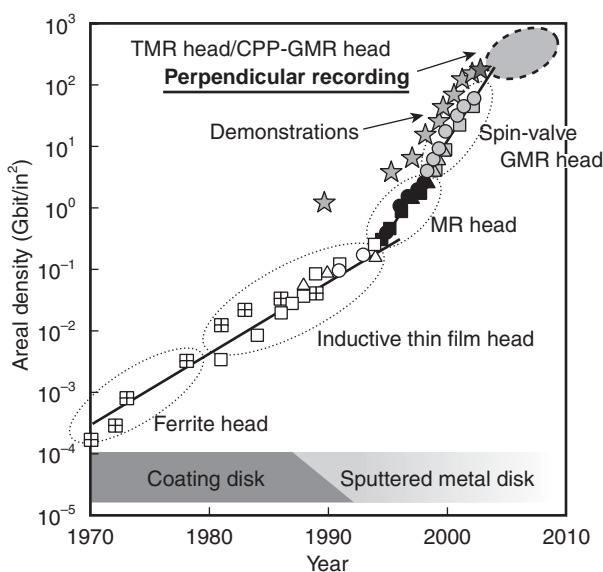


Figure 17
Areal density trends in HDD magnetic recording.

Example measurement results of the MEMS light scanner are shown in **Figure 16**.²⁵⁾ In general, the amount of deformation increases with the acceleration of the MEMS device. However, in this MEMS light scanner²¹⁾ the frame and mirror are separate elements, which is effective for reducing the mirror's dynamic deformation.

6. Future developments

Recent years have seen an increased interest in nanoimprint technology. Because nanoimprint technology²⁶⁾ uses molds to fabricate 3D structures in the nanometer region, advances are being made in its development as a new type of micromachining technology. In the HDD field in particular, where the increase in recording density is considerable (**Figure 17**),²⁷⁾ advances are being made in the development of nanoimprint technology for use in the manufacturing of patterned media²⁸⁾ and discrete track media (DTM),²⁹⁾ which are expected to become the next-generation ultra-high density disk technologies. On the other hand, a vertical sensitivity in the nanometer region has been realized using optical interferometry 3D measurement. However, measurement

sensitivity in the spatial direction has not reached the diffraction limit of light. It should be noted that nanoimprint technology can be used to fabricate structures whose height and spatial dimensions are smaller than the diffraction limit of light and therefore these structures can only be observed using an SEM or atomic force microscope (AFM). Because non-contact, non-destructive, high-speed inspection is indispensable for nanoimprint molds, new breakthroughs in optical measurement technology are being demanded. In the future, we will keep nanoimprint technology in mind as we develop technology for macro-level inspection of array configurations for micro-cyclic structures.

7. Conclusion

In this paper, we introduced the 3D measurement technologies we have developed for semiconductor mounting, HDDs, and light-guiding plates for display elements, as well as an example of a MEMS device application. Innovative manufacturing and measurement technologies have become indispensable in Japan, where calls for strengthened production and demands for leading-edge products that will enable rapid market penetration are increasingly being heard. We will continue our development activities so we can meet these demands.

References

- 1) Fujitsu: Foundry Services.
<http://www.fujitsu.com/downloads/MICRO/fma/pdf/aptbroc.pdf>
- 2) Fujitsu: Hard Drives.
<http://www.fujitsu.com/us/services/computing/storage/hdd/>
- 3) K. Karasawa, T. Nakanishi, and K. Hashimoto: Fluxless Solder Technology with Vapor Phase Soldering in Nitrogen. IMC, Tokyo, 1994, p.11-16.
- 4) Y. Nishiyama, H. Tsukahara, Y. Oshima, F. Takahashi, T. Fuse, and T. Nishino: Development of High-speed 3-D Inspection System for Solder Bumps. SPIE Proceedings, **3306**, 1998, p.60-67.
- 5) T. Fuse, H. Tsukahara, Y. Oshima, Y. Nishiyama, and F. Takahashi: Application of 3-D Sensing Technology to Solder Bump Inspection in Semiconductor Assembly Process. (in Japanese), SII'99, Yokohama, 1999, p.245-248.

- 6) Y. Nishiyama, Y. Oshima, F. Takahashi, T. Fuse, and H. Tsukahara: Development of Hi-Speed Inspection System for Wafer Bumps. (in Japanese), *Mate'99*, Yokohama, 1999, p.67-72.
- 7) Y. Goto, N. Nakamura, A. Mizutani, H. Chiba, and K. Watanabe: Head Disk Interface Technologies for High Recording Density and Reliability. *FUJITSU Sci. Tech. J.*, **42**, 1, p.113-121 (2006).
- 8) J. E. Greivenkamp and J. H. Bruning: Phase Shifting Interferometry. in *Optical Shop Testing*, Second Edition, New York, John Wiley, 1992, p.501-598.
- 9) M. Takeda, H. Ina, and S. Kobayashi: Fourier-Transform method of Fringe-pattern Analysis for Computer-based Topography and Interferometry. *Optical Society of America*, **72**, p.156-160 (1982).
- 10) Y. Nishiyama and H. Tsukahara: Development of Measurement Technique for Magnetic Head Slider ABS using Spatial-carrier Interferometry. (in Japanese), Proc. of ViEW2001, Yokohama, 2001, p.129-134.
- 11) Y. Nishiyama and H. Tsukahara: Measurement Techniques for Magnetic Head Slider ABS. (in Japanese), Proc. of SSII2002, Yokohama, 2002, p.295-300.
- 12) F. Takahashi, T. Fuse, and H. Tsukahara: Development of Micro-waviness Measurement Technique for Magnetic Disks using Spatial-carrier Interferometry. (in Japanese), Proc. of ViEW2001, Yokohama, 2001, p.135-140.
- 13) T. Fuse, F. Takahashi, and H. Tsukahara: Measurement Techniques of Micro-waviness for Magnetic Disks. (in Japanese), Proc. of SSII2002, Yokohama, 2002, p.127-132.
- 14) Y. Y. Chang and J. C. Wyant: Two-wavelength phase shifting interferometry. *Applied Optics*, **34**, p.4539-4543 (1984).
- 15) K. Creath: Step height measurement using two-wavelength phase shifting interferometry. *Applied Optics*, **26**, p.2810-2816 (1987).
- 16) T. Nishikawa, T. Takayasu, and K. Iwata: Measurement of Fine Surface Profile with Two-wavelength Phase-shift Interferometry. (in Japanese), *JSPE*, **57**, 9, p.113-118 (1991).
- 17) T. Nishikawa, T. Fuse, F. Takahashi, and H. Tsukahara: Development of Noncontact Measurement Techniques for LCD Light Guide and Metal Mold. (in Japanese), Proc of Electronics, Information and Systems Conference, Electronics, Information and Systems Society, I.E.E. of Japan, Utsunomiya, 2004, p.761-766.
- 18) Y. Nishiyama, T. Fuse, F. Takahashi, and H. Tsukahara: A Wide Range Measurement Technique using Two Wavelength Phase-shifting Interferometry. (in Japanese), Proc. of ViEW2004, Yokohama, 2004, p.86-91.
- 19) Y. Nishiyama, T. Fuse, F. Takahashi, and H. Tsukahara: Development of Interferometric Microscope using Two Wavelength Phase-shifting Technique. (in Japanese), Proc. of 2005 SOMIT, Yokohama, 2005, p.39-42.
- 20) O. Tsuboi, Y. Mizuno, N. Koma, H. Soneda, H. Okuda, S. Ueda, I. Sawaki, and F. Yamagishi: A Rotational Comb-driven Micromirror with a Large Deflection Angle and Low Drive Voltage. Proc. of MEMS2002, San Diego, 2002, p.532-535.
- 21) O. Tsuboi, X. Mi, N. Kouma, H. Okuda, H. Soneda S. Ueda, and Y. Ikai: A Full-time Accelerated Vertical Comb Drive Micromirror for High Speed 30-Degree Scanning. Proc. of MEMS2004, Maas-tricht, 2004, p.69-72.
- 22) O. Y. Kwon, D. M. Shough, and R. A. Williams: Stroboscopic phase-shifting interferometry. *Opt. Lett.*, **12**, 11, p.855-857 (1987).
- 23) K. Nakano, G. Nishizawa, S. Okuma, K. Hane, and T. Eguchi: Vibration Measurement of Ultrasonic Motor Using Stroboscopic Interferometry. (in Japanese), *JSME-C*, **62**, 598, p.2237-2243 (1996).
- 24) M. R. Hart, R. A. Conant, K. Y. Lau, and R. S. Muller: Stroboscopic Interferometer System for Dynamic MEMS Characterization. *J. Microelectromechanical Syst.*, **9**, 4, p.409-418 (2000).
- 25) F. Takahashi and H. Tsukahara: Motion analysis of MEMS micromirror using stroboscopic phase-shift interferometer. (in Japanese), Proc. of SSII2006, Yokohama, 2006, p.350-353.
- 26) S. Y. Chou, P.R. Krauss, and P.J. Renstrom: Imprint of sub-25 nm vias and trenches in polymers. *Appl. Phys. Lett.*, **67**, 21, p.3114-3116 (1995).
- 27) I. Kaitsu, R. Inamura, J. Toda, and T. Morita: Ultra High Density Perpendicular Magnetic Recording Technologies. *FUJITSU Sci. Tech. J.*, **42**, 1, p.122-130 (2006).
- 28) S. Y. Chou, M. Wei, P. R. Krauss, and P. B. Fischer: Study of nanoscale magnetic structures fabricated using electron-beam lithography and quantum magnetic disk. *Journal of American Vacuum Society*, **12**, 6, P.3695-3698 (1994).
- 29) S. E. Lambert, I. L. Sanders, and M. T. Krounbi: Recording characteristics of submicron discrete magnetic tracks. *IEEE Trans. Magn.*, **Mag-23**, 5, p.3690-3692 (1987).



Hiroyuki Tsukahara, Fujitsu Laboratories Ltd.

Mr. Tsukahara received the B.S. degree in Communication Engineering from the University of Electro-Communications, Tokyo, Japan in 1981. He joined Fujitsu Laboratories Ltd., Kawasaki, Japan in 1981, where he has been engaged in research and development of sensing technology and image processing. He is a member of the

Institute of Electronics, Information and Communication Engineers (IEICE) of Japan.